

Fig. 1. Configuration of the shock and rarefaction waves produced by passage of a shock wave from the lower surface of the sample. Arrows show the geometrical relationship between the rarefaction wave velocity V , the particle velocity u_p , and the shock front velocity U_s .

The first rarefaction signal to reach an interior point is that propagating from the lower corners of the crystal. Simple geometrical relations (Figure 1) then give the rarefaction velocity V as

$$V = U_s [\tan^2 \alpha + (U_s - u_p)^2 / U_s^2]^{1/2} \quad (1)$$

where U_s is the shock front velocity, u_p is the particle velocity, and α is the angle between the side of the sample and the locus of intersection of the shock and rarefaction waves (Figure 1).

The sample is mounted on a tungsten 'driver plate' that is struck by a tungsten 'flyer plate' mounted in the tip of the projectile. The pressure P and particle velocity in the sample are determined by impedance matching [e.g., Rice *et al.*, 1958], using the measured projectile velocities and P - u_p curves for tungsten [McQueen

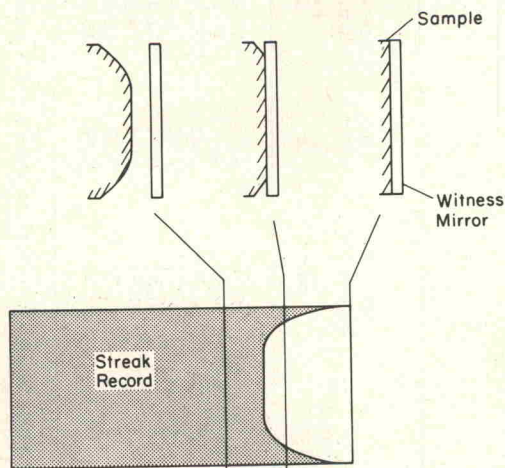


Fig. 2. Schematic illustration of the recording by the streak camera of the impact of the sample on the witness mirror.

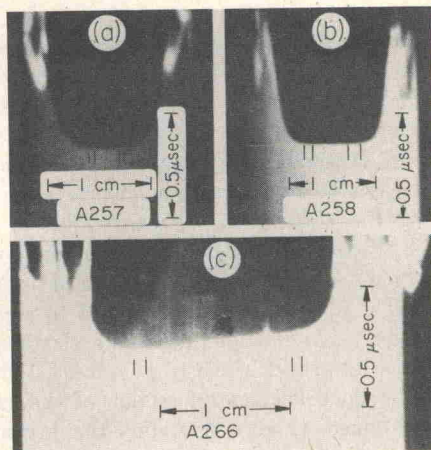


Fig. 3. Streak records of sample-mirror impacts. Length (horizontal) and time (vertical) scales are indicated. Numbers refer to shot numbers (Table 1). Initial mirror-sample separations were (a) 0.76 mm, (b) 0.13 mm, (c) 0.25 mm. Samples *a* and *b* were polycrystalline, and sample *c* was single crystal.

et al., 1970] and MgO [Carter *et al.*, 1971]. The shock velocity is then calculated from the Rankine-Hugoniot relation

$$U_s = P / \rho_0 u_p \quad (2)$$

where ρ_0 is the zero-pressure density of the sample.

The MgO samples used in this study were five polycrystalline samples supplied by T. Vasilos of the Avco Corporation and three single crystals with (100) cleavage faces purchased from the Norton Research Corporation. The polycrystalline samples described and measured ultrasonically by Schreiber and Anderson [1968] and Spetzler [1970] were obtained from the same source.

RESULTS

A basic difficulty of this method is the emergent nature of the edge effect (Figure 3). Initial experiments were therefore performed with the mirror spaced a small distance (0.76 mm) from the sample surface. This spacing allows the contrast in free surface velocities across the sample to amplify the contrast in the total transit time, which is the sum of the shock wave transit time through the sample and the free surface transit time to the mirror. Sample specifications and results for four such shots are

given in Table 1. Figure 3a (shot A257) is a typical record. Since there was not a really well-defined flat central section of the cutoff in these records (variations of light extinction over 10 nsec existed over the central 2 mm of the sample), it was thought that some deformation of the sample free surface might be occurring during the transit. To test this idea, a shot (A258, Figure 3b and Table 1) was fired with the mirror-sample separation reduced to 0.13 mm. (The spacing was not reduced to zero to avoid any complications from the elastic precursor to the shock wave [e.g., Ahrens, 1966].) A well-defined flat central section of the cutoff was obtained (Figure 3b), but the measured rarefaction velocity was considerably lower than that in the previous shots (Table 1). The remaining three shots were fired on the single-crystal samples with intermediate mirror-sample spacing (0.25 mm). Results are given in Table 1 and Figure 3c and exhibit rarefaction velocities intermediate between those of the previous shots. (The origin of the low-angle irregularities in shot A266, shown in Figure 3c, which were also observed in the other single-crystal shots, is unknown. Some uncertainty in the extent of the edge effect results from their presence.)

DISCUSSION

An interpretation of these observations is suggested by the observations of other workers. *Altshuler et al.* [1960] observed that the edge effect had a much sharper beginning for shocked liquids than for shocked solids and that the measured rarefaction velocities corresponded closely to the hydrodynamic (bulk) sound speeds for the liquids but that for the solids they were higher and corresponded more closely to the expected longitudinal elastic velocities of the solids. *Kusubov and van Thiel* [1969] observed the decompression of 6061-T4 aluminum directly using manganin pressure gages and found that the decompression occurred in two stages, the first stage propagating at about the velocity of longitudinal elastic waves and the second stage, identified by an increase in the rate of decompression, propagating at about the bulk sound speed of aluminum. These observations were interpreted in terms of a two-stage elastoplastic decompression, in which the decompression is one dimensional and elastic until a critical deviatoric stress is reached, after

TABLE 1. MgO Rarefaction Velocity Data

Shot No.	Sample Type*	Mirror Separation z , mm	Edge Effect x , mm	Sample Dimension y , mm	Sample Dimension h , mm	tan α	Tungsten Projectile Velocity V_{TP} , km/sec	Rarefaction Velocity V_r , km/sec	Shock State		
									Pressure P_r , kb	Density ρ_r , g/cm ³	Temperature T_r , °K
A250	P	0.76	4.29	11.43	3.81	1.13	1.95	12.0	446	4.31	570
A252	P	0.76	4.37	11.40	3.81	1.14	2.25	12.4	528	4.41	650
A257	P	0.76	4.42	11.46	3.86	1.14	1.50	11.7	326	4.10	475
A261	P	0.76	2.92	11.43	2.49	1.18	1.60	12.0	353	4.19	490
A258	P	0.13	2.46	11.43	3.83	0.64	1.55	8.8	340	4.17	480
A263	S	0.25	5.18	19.80	5.28	0.98	2.02	11.1	465	4.34	590
A266	S	0.25	3.94	19.20	4.62	0.85	2.25	10.4	528	4.41	650
A267	S	0.25	4.72	18.82	4.54	1.04	2.20	11.6	514	4.40	630

*P represents the polycrystalline sample and S represents the single-crystal sample.